

Hyperbaric oxygen treatment increases intestinal stem cell proliferation through mTORc1 signaling in *Mus musculus*

Ignacio Casanova

Universidad de Chile <https://orcid.org/0000-0001-9502-570X>

Isaac Peña-Villalobos

University of Chile: Universidad de Chile

David Arancibia-Altamirano

University of Chile: Universidad de Chile

Pablo Lois

Mayor University: Universidad Mayor

Verónica Palma (✉ vpalma@uchile.cl)

University of Chile: Universidad de Chile

Research

Keywords: Intestinal stem cells, Hyperbaric oxygen treatment, mTORc1, proliferation, rapamycin

Posted Date: November 20th, 2020

DOI: <https://doi.org/10.21203/rs.3.rs-108513/v1>

License:   This work is licensed under a Creative Commons Attribution 4.0 International License.

[Read Full License](#)

1 Hyperbaric oxygen treatment increases intestinal stem cell proliferation through mTORc1 signaling
2 in *Mus musculus*

3

4

5 Ignacio Casanova-Maldonado¹, Isaac Peña-Villalobos¹, David Arancibia¹, Pablo Lois^{1,2} and
6 Verónica Palma^{1*}

7

8 1. Laboratory of Stem Cells and Developmental Biology, Faculty of Sciences. Universidad de
9 Chile. Santiago, Chile.

10 2. Present address: Postgraduate in Education Department; Faculty of Humanities,
11 Universidad Mayor

12

13

14

15 * Corresponding Author: Verónica Palma (vpalma@uchile.cl), Phone number (56-2) 2978 7221. Las
16 Encinas 3370. Milenio Building Floor 3, Ñuñoa, Santiago, Chile. 7800024

17

18

19

20

21

22

23

24

25

26

27

28

29

30

31

32

33 **Abbreviations:** Hyperbaric oxygen treatment (HBOT), mTOR complex 1 (mTORc1), intestinal
34 stem cells (ISCs), caloric restriction (CR), columnar base cells (CBC), Bromodeoxyuridine (BrdU),
35 phospho-Histone H3 (PHH3), cytochrome c oxidase (COX), citrate synthase (CS),
36 immunofluorescence (IF), immunohistochemistry (IHC)

37

38

39 **Abstract**

40

41 **Background:** Hyperbaric oxygen treatment (HBOT) has been used for more than a decade to treat
42 diverse diseases like diabetic foot ulcers and ischemic injuries. More recently, HBOT has been
43 reported to modulate proliferation of neural and intestinal stem cell populations, but the molecular
44 mechanisms underlying these effects are not completely understood.

45 **Objective:** In this study we aimed to determine HBOT stem cell modulation by evaluating in
46 particular the role of the mTOR complex 1 (mTORc1), a key regulator of cell metabolism that
47 modifies its activity depending on oxygen levels, as a potential mediator of HBOT in murine intestinal
48 stem cells (ISCs).

49 **Methods:** Mice were exposed to 10 or 20 HBOT sessions and the proliferation of the ISCs were
50 analyzed by immunofluorescence or immunohistochemistry using the specific ISCs marker, Olfm4.
51 The regulation of HBOT and mTORc1 pathway was analyzed through S6K1 phosphorylation by
52 western-blot and through the inhibition by rapamycin.

53 **Results:** We discovered that acute HBOT can increase proliferation of ISCs in a synchronous fashion
54 without affecting the animal's oxidative metabolism. Noteworthy, the mTORc1 inhibitor rapamycin
55 also increases the proliferation of ISCs. This effect has been attributed to its capacity to mimic a
56 caloric restriction (CR). Interestingly, the combination of HBOT and rapamycin does not have a
57 synergic effect. Nevertheless, HBOT can recover rapamycin induced mTORc1 inhibition, possibly
58 acting through a competitive modulation on mTORC1.

59 **Conclusions:** Collectively, our results suggest that HBOT proliferative effect on ISCs is modulated
60 by mTORc1 signaling representing a promising new approach to treat intestinal conditions.

61

62 **Keywords:** Intestinal stem cells, Hyperbaric oxygen treatment, mTORc1, proliferation, rapamycin.

63 **Introduction**

64 Hyperbaric oxygen treatment (HBOT) consists in administration of oxygen at high pressures. HBOT
65 works under Henry's law that states that the amount of gas dissolved in a liquid is proportional to the
66 partial pressure that the gas applies over such liquid. As a result, the amount of oxygen dissolved in
67 blood increases, which causes a systemic effect by enriching tissues in oxygen through the
68 bloodstream.

69 HBOT is widely used as an adjuvant treatment to treat diabetic foot ulcers (Kalani et al; 2002), brain
70 injuries (Zhang et al; 2010 and Bennett et al; 2012) and to promote wound healing (Eskes et al; 2011
71 and Kranke et al; 2015 and Peña-Villalobos et al; 2018). Recent studies have proposed that its effects
72 on wound healing occurs due modulation of HIF-1 α (Sunkari et al; 2015) and Vascular Endothelial
73 Growth Factor (VEGF) (Lee et al; 2006) signaling pathways. Nonetheless, the mechanisms are under
74 continuous debate and still far from being fully understood.

75 In the last decade, studies have focused on stem cells as cellular targets of HBOT, revealing positive
76 effects on proliferation and regeneration on both neural (Zhang et al; 2011) and mesenchymal stem
77 cell populations (Dhar et al; 2012). An interesting niche for studying the effects of HBOT on stem
78 cell proliferation is the intestinal epithelium, the most vigorously self-renewing
79 tissue of adult mammals (Snippert et al; 2010). Within this epithelium, intestinal stem cells (ISCs)
80 reside at the base of the crypts of Lieberkühn, allowing the generation of absorptive or secretory
81 progenitors who migrate toward the tip of the villus (Barker et al; 2014), regenerating the small
82 intestine every 3 days in mice (Totafurno et al; 1987 and Clevers; 2013). The crypts of Lieberkühn
83 have been well studied and characterized in terms of their cellular composition. ISCs are also named
84 columnar base cells (CBC) for their position in the base of the crypts and can be identified by the
85 expression of specific markers like Lgr5 (a membrane protein) or Olfm4 (a cytoplasmatic protein).
86 CBCs give rise to another functionally distinct population of stem cells, called +4 (due to their
87 position in the crypt) or emergency stem cells. The complex nature of ISCs is becoming clear in recent

88 years, revealing a hierarchy between Lgr5+ and +4 under homeostasis and stress responses (De Mey
89 & Freund; 2013 and Basak et al; 2017).

90 The homeostatic renewal in the intestinal epithelium is commanded by oxidative metabolism and
91 guided by the mTOR complex 1 (mTORc1), a macromolecular nutrient- and growth factor-responsive
92 kinase (Yilmaz et al; 2012 and Sampson et al; 2015). The kinase1 is also able to integrate a response
93 to transcription factors (Igarashi et al; 2016) and oxygen (Schieke et al; 2006 and Saxton & Sabatini;
94 2017). mTORc1 signaling involves the activation of many proteins like 4E-BP1 and S6K1 through
95 phosphorylation, regulating cellular anabolic growth and proliferation (Fingar et al; 2002). A plethora
96 of studies have shown that this complex can be inhibited by the administration of rapamycin, an
97 allosteric inhibitor (Benjamin et al; 2011), preventing the formation of the complex and therefore
98 downregulating the signaling pathway (Fingar et al; 2004). Furthermore, rapamycin has been used to
99 mimic the effects of a caloric restriction (CR), resulting in an increase of lifespan in different species
100 like yeast, mice and humans (Cox et al; 2009, Dai et al; 2014 and Wang et al; 2017).

101 The regulatory mechanisms that control ISCs in response to HBOT are just beginning to be explored.
102 Here we analyzed the effects of acute HBOT on the ISCs proliferation rates of *Mus musculus* small
103 intestine and its modulation by mTORc1. First, we established the number of HBOT sessions required
104 to promote a positive effect on ISCs proliferation. Secondly, we sought to understand the complex
105 relation between oxygen tension and proliferation, mediated by the mTOR complex. Our results show
106 that animals treated for 10 days with HBOT present a trend to increase ISCs proliferation. However,
107 animals treated with a daily HBOT session for 20 consecutive days show an increase in proliferation
108 in a synchronous fashion among crypts. Noteworthy, although animals treated with rapamycin also
109 increase the number of ISC proliferating by crypt, mimicking the effects of a CR (Cox et al; 2009 and
110 Dai et al; 2014), a combined treatment with HBOT and rapamycin did not increase ISC proliferation.
111 We speculate that the latter is probably due a competition for mTORc1. Strikingly, we found that
112 HBOT can recover the inhibition of rapamycin over mTORC1. Overall, our findings suggest that

113 HBOT can replicate the effects of a CR, stimulating proliferation of ISCs. As such, we propose that

114 HBOT could be a potential adjuvant treatment for intestinal injuries and pathologies.

115

116 **Methods**

117 *Animals*

118 Forty-six adult (3 months old) males of the BALB/c strain of *Mus musculus* were obtained from the
119 central animal housing facilities at the Faculty of Sciences. All animal procedures were in accordance
120 with the Chilean legislation and were approved by Institutional Animal Care and Use Committee
121 (CICUA) at the Universidad de Chile.

122 To analyze the effects of HBOT on ISCs proliferation we generated four groups: Control group for
123 ten days (C10D), HBOT group for ten days (H10D), Control group for twenty days (C20D) and
124 HBOT for twenty days (H20D) (Table I). Each group was formed by five animals, considering no
125 siblings in the same group. They were housed with their siblings but properly identified and kept in
126 a temperature-controlled room, maintained at $25^{\circ} \pm 1$ °C in a LD= 12:12 cycle, with food and water
127 *ad libitum*.

128 In order to explore the relationship of HBOT with mTORC1 signaling we generated another set of 4
129 experimental groups: 2 Groups without HBOT sessions but injected with rapamycin (Rapa Ctrl) or
130 with DMSO (vehicle of rapamycin) (DMSO Ctrl), and 2 groups treated with HBOT injected with
131 rapamycin (RAPA HBOT) or with DMSO (DMSO HBOT) (Table II). All groups were treated for 20
132 consecutive days. Each group included five animals, maintained in the same conditions as described
133 above.

134 Table I: Animal groups generated for analysis of HBOT impact on ISCs proliferation.

ISCs proliferation		
	10 Days	20 Days
Control	C10D	C20D
HBOT	H10D	H20D

135

136 Table II: Animal groups generated for the study of the relationship between HBOT, mTORC1
137 pathway and ISCs proliferation.

mTOR and ISCs		
	Control	HBOT
DMSO	DMSO Ctrl	DMSO HBOT
rapamycin	Rapa Ctrl	Rapa HBOT

138

139 *HBOT sessions*

140 HBOT was performed in a 19.56 L experimental chamber at 25°C (Osorio Hermanos & Cia. Ltd.,
141 Quillota, Chile). Animals were placed in individual cages, then the remaining air inside the chamber
142 was replaced with 100% O₂ while the pressure was increased for 15 minutes until 2.0 ATA (absolute
143 atmospheres) were reached. The latter conditions were maintained for 1.0 h followed by
144 decompression from 2.0 ATA to atmospheric pressure gradually for other 15 min (figure 1A).
145 Therefore, each session took 1.5 h (Dave et al; 2003 and Peña-Villalobos et al; 2018).

146 *Rapamycin administration*

147 Rapamycin (Calbiochem, 553210) was dissolved in DMSO (5 mg/125 µl) and diluted in PBS 1X
148 1:100 v/v. Every other day rapamycin was injected intraperitoneally (2 mg/kg), always at the same
149 hour and before starting the HBOT session.

150 *Intestinal tissue dissection*

151 After the last HBOT session animals were injected intraperitoneally with 800 µl of 20 mg/ml BrdU
152 (Sigma-Aldrich). One hour later the animals were sacrificed by cervical dislocation. Immediately the
153 entire digestive tract was dissected on a cooled surface and the intestine contents were gently removed
154 mechanically. Next, the first third of the small intestine (duodenum) was cut longitudinally and used
155 for histological analysis. This segment was fixed in 4% PFA (Sigma-Aldrich) for 2 h at 4°C followed
156 by dehydration overnight (O.N) in 30% sucrose (Merck) solution. Tissues were embedded in OCT

157 (Tissue-Tek), placed in a disposable vinyl specimen mold (Tissue-Tek Cryomold) and stored at -80°C
158 until further use.

159 *Immunostaining*

160 To realize immunofluorescence (IF) and immunohistochemistry (IHC) we followed the exact same
161 protocol of Peña-Villalobos et al. (2018). Briefly, slides of either 14 and 7 µm thickness were prepared
162 with the epitope-unmasking protocol and incubated overnight at 4°C with 1:100 monoclonal mouse
163 Anti-Bromodeoxyuridine Clone Bu20a (BrdU, Dako, M0744) primary antibody or 1:400 monoclonal
164 rabbit Anti-Olfm4 (Cell Signaling, 39141). For IF, we used 1:500 goat anti mouse Alexa 555 (Life
165 technology, A21424) as a secondary antibody to BrdU and 1:500 goat anti rabbit Alexa 488 (Life
166 technology, A11034) as a secondary to Olfm4. DAPI (Invitrogen) was used to label nuclei. For IHC,
167 we used hematoxylin/eosin (H&E) and DAB staining as described in Peña-Villalobos et al. (2018).
168 To analyze the IHC, an optical microscope (Olympus BX51) at 40X and 100X equipped with a digital
169 camera (Moticam 2500) was used whereas for IF a confocal microscope (Zeiss 710) was used. Z-
170 stacks and image analysis was made by ImageJ and FIJI programs. Figures were created by
171 Biorender.com.

172 *Enzyme Assays*

173 The duodenum was homogenized in 10 volumes of phosphate buffer 0.1 M with EDTA 0,002 M (pH
174 7.3) with an Ultra Turrax homogenizer (20,000 rpm) on ice. Samples were sonicated for 45 seconds
175 on ice using an Ultrasonic Processor VCX 130. Cellular debris was removed by centrifugation for 15
176 min at 12,000 G at 4°C. Then the supernatant was isolated and used for determination of protein
177 concentration by Bradford method.

178 Citrate Synthase and Cytochrome C Oxidase activity were determined spectrophotometrically
179 according to Peña-Villalobos et al. 2018.

180

181 *Western Blot*

182 Homogenized duodenums, stored at -80°C with proteases and phosphatases inhibitors, were left on
183 ice for 1 h. 50 µg of the sample was loaded on acrylamide gel posterior to Lowry quantification (550
184 nm; Tecan M200) and then transferred to a nitrocellulose film. The film then was treated with BSA
185 5% in TBS-T 0,1% for an hour, washed in PBS and incubated for 12 h with anti-phospho p70 S6K1
186 (Thr389) (1:1000, Cell signaling) or anti-p70 S6K1 (1:1000, Cell signaling) and anti-β actine (1:
187 5000, Cell Signaling). For protein detection we used Rabbit anti-mouse HRP (1:5000; Cell signaling)
188 to identify p70 S6K1 and p70 S6K1 phosphorylated and Mouse anti-β actine (1:5000, Cell Signaling)
189 with luminol. X-ray films were obtained after 1 h exposition in dark room for S6K1 and S6K1-P,
190 while β actine detection last 10 seconds of exposition.

191 *Statistical analysis*

192 The number of positive labeled cells per villus of each crypt were scored by two independent counters.
193 To determinate if HBOT has effects on the proliferation dynamics of ISCs we counted the number of
194 BrdU+ cells in 36 randomly chosen crypts from the first third of the intestine of each individual (n=3
195 per treatment). For IF, ISCs positive cells were considered only if they expressed the specific marker
196 Olfm4 (Olfm4+ cells). Permutation test was performed in R software, using a permutation test script
197 of 1000 permutation for each analysis. Data from mTOR inhibition by rapamycin and western blot
198 were also analyzed by permutation test. To analyze the distribution of the data we used a
199 Kolmogorov-Smirnov test. As for the first experiment (HBOT for either 10 or 20 days) we considered
200 a Bonferroni correction, having an $\alpha= 0.0125$.

201

202 **Results**

203 *HBOT increases ISC proliferation in a synchronous fashion*

204 Stem cells *in vivo* reside in a dynamic and specialized microenvironment, the so- called niche. The
205 stem cell niche is influenced by a variety of factors including physical and metabolic parameters.
206 Oxygen tension is known to be an important cellular input modulating stem cell self-renewal and
207 differentiation potential. Thus, many stem cells, including ISCs, respond actively to changes in
208 oxygen tension.

209 ISCs are located at the bottom of the intestinal crypt and can be identified as Olfm4+ cells, revealing
210 a co-distribution with the BrdU label (figure 1 B-E). To determine the proliferation effects of HBOT
211 on ISCs, we evaluated the number of BrdU+ cells per crypt in all experimental groups. Only small
212 intestines from mice treated with HBOT for 20 days (H20D) show an increment in the number of
213 BrdU+ cells (figure 1 F-J). Interestingly, another cell population, located at near position to the
214 intestinal crypts, also exhibited BrdU staining (figure 1E). Hence, we cannot discard that HBOT has
215 effects on another cell population, besides the Olfm4+ CBC pool.

216 HBOT increased proliferation of cells within the crypts in a synchronous way. This was determined
217 by calculating the stabilization coefficient (figure 1K) for each group. H20D was the only group that
218 shows clear differences. To evaluate if this synchronization in proliferation was generated by a
219 possible arrest in the cell cycle due to treatment, we analyzed the ratio between BrdU and PHH3
220 positive cells in intestinal samples from C20D group or H20D group (data not shown). We did not
221 find differences in these ratios. Hence, we conclude that HBOT does not generate this synchronization
222 of proliferation due to a cell cycle arrest in ISCs.

223 *HBOT has an accumulative effect in time*

224 The frequency distribution from groups treated with H10D was different from its control C10D
225 despite not showing differences in the numbers of BrdU+ cells per crypts. When we analyzed the

226 frequency distribution for each group (figure 2), we found that only control groups showed no
227 differences ($p= 0.796$). Interestingly, the frequency distribution from H10D was different, both from
228 the control groups and H20D, indicating that, despite not showing significant differences in the
229 number of BrdU+ cells per crypt (figure 1J), H10D already generates a change in the proliferation
230 behavior of the ISCs.

231 *Acute HBOT does not change enzymatic activity in the small intestine*

232 Intestines from H20D did not show differences in comparison to their control in the enzymatic activity
233 related to oxidative metabolism. We sought to analyze if the increment in the proliferation of the ISCs
234 by HBOT could be explained by an increase in the activity of cytochrome c oxidase (COX) and citrate
235 synthase (CS), both enzymes related with aerobic ATP generation. To this end, we analyzed the
236 activity of these enzymes in the whole duodenum in each experimental group (figure 3A). No
237 difference was found in the activity of both enzymes, when analyzed per gram, total in tissue or total
238 protein between control (C10D and C20D) and both HBOT groups (figure 3B-C). Therefore, HBOT
239 effects must encompass another molecular pathway to account for its effect.

240 *HBOT modulates proliferation of the ISCs through mTORC1 pathway activation*

241 To evaluate if HBOT could activate the mTOR pathway, capable of sensing changes in oxygen levels,
242 we generated four groups, combining rapamycin with or without HBOT (see table II). In line with
243 the literature, animals treated with rapamycin showed a mTORc1 pathway suppression as revealed
244 by the lack of phosphorylation on S6K1 (figure 4A; supplementary figure 1). On the other hand,
245 animals injected with rapamycin vehicle (DMSO) showed no inhibition on the phosphorylation status
246 of S6K1, either with or without HBOT. Stunningly, animals that received a combined treatment with
247 rapamycin and HBOT revealed strong phosphorylation on S6K1 (Figure 4B). Therefore, we suggest
248 that HBOT can recover rapamycin inhibition of mTOR pathway signaling.

249 Acute HBOT can simulate the effects on ISCs proliferation generated by a CR. When we compared
250 the effects on ISCs proliferation of rapamycin (Rapa Ctrl) and HBOT for 20 days (DMSO HBOT),
251 we found that each treatment increases the number of BrdU+ cells per crypt (figure 5 A-E).
252 Nevertheless, animals treated with both HBOT and rapamycin (Rapa HBOT) show no increase in
253 ISC proliferation.

254 Finally, a careful analysis of frequency distribution of BrdU+ cells per crypt indicated that only 2
255 comparisons present no differences. Rapa HBOT and DMSO Ctrl groups exhibited no differences
256 (figure 6F) while Rapa Ctrl and DMSO HBOT groups also showed no differences in their
257 distributions (figure 6G). These data, in combination with the results presented in figure 5E, suggest
258 that HBOT has the same effects on ISCs proliferation as a CR generated by rapamycin.

259

260

261

262

263

264

265

266

267

268

269

270

271 **Discussion**

272 HBOT has been reported to modulate the stem cells proliferative behavior in two well-known adult
273 stem cell niches, in the bone marrow (Geng et al; 2015) and the brain (Wang et al; 2007). In this
274 work, we demonstrate that HBOT also can enhance the proliferation of ISCs in a synchronous fashion.
275 Moreover, we provide findings that this proliferative effect is mediated by mTORc1 signaling.

276 Nearly 90% of the intestinal epithelium is replaced every 3–4 days by cells newly generated from the
277 crypt epithelium. However, long-lived ISCs harbor in the crypt bottom to replenish the large amount
278 of disposable functional epithelium. ISCs produce rapidly cycling progenitor cells that migrate up the
279 crypt-villus axis and differentiate into mature epithelial cells that are eventually shed off into the
280 lumen. Small intestine partial pressure of oxygen (PO₂) values have been reported to be 2–5%, 3–
281 6% and 5–9% O₂ for lumen, mucosa and serosa layers, respectively (Espey; 2013).

282 To explore whether oxygen tension impacts cellular turnover in the small intestine, we used an
283 established HBOT protocol (Peña-Villalobos et al; 2018). In our previous work, rodents were
284 exposed to HBOT conditions in ten consecutive sessions. We did not find a significant effect of
285 HBOT on cell proliferation, as all groups had similar numbers of BrdU+ cells per crypt. But in the
286 present work, increasing the time length of treatment by applying HBOT for 20 consecutive days lead
287 to a significant cell proliferation rise within the crypts. The effect of HBOT is clearly observable on
288 day 20 but had an accumulative effect that was already evidenced since day 10. The analysis of the
289 frequency distribution of BrdU+ positive cells from C10D with H10D groups indicates that despite
290 showing no differences in the number of BrdU+ cells per crypts (figure 1J), there are differences in
291 the frequency of proliferative cells (figure 2). The latter indicating that HBOT for 10 consecutive
292 days already generates a change in the proliferation dynamics of the ISCs within the crypts.

293 Using the specific ISCs marker, Olfm4, we observed that stem cells co-distribute with the
294 proliferation marker BrdU. Of note, another cell population shows proliferative labeling but no
295 Olfm4 staining (figure 1E). Thus, we cannot discard the possibility that HBOT can stimulate

296 proliferation of progenitor cells and/or emergency ISCs. The recruitment of these cells together with
297 ISCs would represent an interesting broader effect of HBOT. Keeping in mind that HBOT has
298 recently reported to increase the proliferation of progenitor cells *in vitro* (Benincasa et al; 2019), our
299 result would be the first in describing similar results *in vivo* in the intestinal niche. On the other hand,
300 if, in addition, the target of acute HBOT are the so-called emergency ISCs, a population that has been
301 described as quiescent (Muñoz et al; 2012), this could mean that the treatment can promote their
302 recruitment to ISCs. The possible relationship between the quiescent and the actively cycling ISCs
303 and the biological consequences of their HBOT response needs to be further explored.

304 The increase in proliferation in H20D occurred in a synchronous fashion (figure 1K). This means that
305 along the duodenum all the H20D crypts presented a similar and higher number of BrdU+ cells than
306 the control or H10D groups. This synchronicity could emerge as a consequence of cell cycle arrest
307 provoked by HBOT or by the maximization of the proliferative capacity of the crypt's cells. As shown
308 by previous authors, identification of the BrdU and PHH3 proportion allows for evaluation of cell
309 cycle arrest (Cappella et al; 2008 and Ren et al; 2018). Based on these works we analyzed the
310 proportion of the aforementioned markers in the C20D and H20D groups and determined that HBOT
311 does not arrest the cells in a particular stage of the cell cycle. Thus, HBOT maximizes the proliferation
312 mode in the intestinal crypts.

313 It is critical to note that these effects were not generated by an increase in ATP production due to an
314 enhanced oxidative metabolism by an increment in available oxygen, as revealed by the analysis of
315 the enzymatic activity of COX and CS (figure 3 B-C). These results were in concordance with our
316 previous work, where we showed that using HBOT for 10 consecutive days did not change the basal
317 metabolic rates of mice (Peña-Villalobos et al; 2018). They are also in line with a recent *in vitro*
318 analysis of lung fibroblast where no changes in CS activity were reported (Dejmek et al; 2018).
319 Notwithstanding, it is remarkable how a treatment that increases oxygen tension does not alter
320 oxidative metabolism in the intestinal epithelium while other reports indicate that acute HBOT does

321 generate changes in tissues like brain or skeletal muscle (Matchett et al; 2009 and Ishihara; 2019). If
322 HBOT can generate a differential physiological response in tissues and organs warrants further
323 investigation.

324 mTORC1 is known to sense oxygen levels (Lane et al; 2017) and to regulate stem cell proliferation
325 (Murakami et al; 2004 and Hu et al; 2017). The stimulation of S6K1 by mTORC1 has been widely
326 reported. In addition, mTORC1 has been characterized as a rapamycin sensitive complex. Strikingly,
327 we found that HBOT can recover rapamycin induced mTOR pathway inhibition, as shown in figure
328 4A and supplementary figure 1. Furthermore, analysis of BrdU+ cells per crypt showed that HBOT
329 and rapamycin increased proliferation of the cells within the crypt independently. We attribute this
330 effect of rapamycin to its capacity to mimic a CR. Under CR, Paneth cells, forming part of the stem
331 cell niche, sense a downregulation of mTORC1 and generate a paracrine signal (NAD synthesis)
332 stimulating ISCs to proliferate (Igarashi & Guarente; 2016 and Peña-Villalobos et al; 2019). HBOT
333 also increases proliferation through mTORC1, but, at this point, we would like to suggest that it
334 probably occurs through a different and competitive way of rapamycin's action. When both
335 treatments are combined, there is no increase or synergic effect between them. On the contrary, they
336 cancel each other's effects (figure 4), resulting in no differences in the number of BrdU+ cells per
337 crypt and the frequency distribution of ISCs (figure 5A, 6F). Therefore, HBOT can modulate the
338 proliferation of ISCs (and most likely progenitor cells) in the crypt acting through mTOR pathway
339 signaling. The possible intricate network of the interplay between these two metabolic mTORC1
340 stimuli with similar output warrants further investigation.

341 The intrinsic metabolism of adult stem cells that reside in a hypoxic condition like neural stem cells
342 in the subventricular zone or mesenchymal stromal cells in the bone marrow seems to be maintained
343 by an aerobic glycolysis but without generating high levels of reactive oxygen species (ROS) and
344 therefore maintaining a low proliferation rate that preserves the self-renewal potential (Shyh-Chang
345 & Ng; 2017). But when these cells sense a high ROS environment, they undergo an active

346 proliferation and differentiation process (Tothova et al; 2007). In *Drosophila*, ISCs also undergo
347 hyperproliferation in response to high ROS levels (Hochmuth et al; 2011). This high ROS level can
348 be produced by an increase in mitochondrial activity which in turn can be activated by an increase in
349 mTOR signaling. On the other hand, it has been proposed that changes in the REDOX state of stem
350 cells, induced by changes in the electron transport chain due oxygen reduction, can change their
351 proliferative behavior and might have effects at nuclear epigenetic and gene expression (Wei et al;
352 2018). Therefore, the increase in ISCs proliferation in mice could be explained by a response to an
353 increase in ROS levels or changes in REDOX state. Our group is currently investigating the
354 relationship between HIF1- α , ROS levels and mTORC1 as a candidate mechanism to explain the
355 effects in response to hyperbaric oxygen.

356 The metabolic program of stem cells is intrinsically determined and essential for the maintenance of
357 those cells, impacting the balance of self- renewal, and differentiation. HBOT has positive effects in
358 bone marrow stem cells migration and mesenchymal stem cells proliferation (Thom et al; 2006 and
359 Geng et al; 2015). Here we show that HBOT can be also used to increase the proliferation of ISCs
360 and progenitor cells through mTORc1 pathway signaling, without altering the oxidative metabolism
361 of the animal's small intestine. Results in line with recent findings pointing to the capacity of
362 mTORc1 to regulate the proliferation state of post-natal skeletal stem cells (Newton et al; 2019). Most
363 likely, since HBOT promotes a systemic effect and other tissue-resident stem cell pools are affected.
364 Future studies need to address a possible HBOT/mTORC1 signaling on other somatic stem cells
365 populations.

366 In summary, our findings indicate that HBOT on its own can mimic the effects of rapamycin on
367 proliferation of ISCs. Noteworthy, HBOT has the advantage of being a non-invasive and relatively
368 cheap treatment, favoring its use in future therapies to regenerate damaged intestinal epithelia.

369

370 **Conclusions**

371 HBOT for 20 consecutive days potentiates ISC proliferative behavior, such increase in proliferation
372 occurs in a synchronous fashion all along the duodenum without altering oxidative metabolism,
373 suggesting that HBOT maximizes the proliferation rate of ISC. Our results show that mTORC1
374 pathway modulation is responsible for this HBOT driven increase in proliferation. When mTORC1
375 is inhibited by rapamycin, ISCs undergo a caloric restriction like situation, that in mice generates
376 similar effect to that observed if they had been treated with HBOT for 20 consecutive days. However,
377 when both treatments were combined, no effect on ISC proliferation were detected, suggesting that
378 HBOT effect were modulates through mTORC1 pathway, and due its inhibition, the effect disappears.
379 These results shed light on the molecular mechanisms underlying HBOT therapeutic action, a medical
380 treatment that has been used for a long time but whose subjacent mechanisms remain unclear.

381 **Acknowledgments**

382 The authors would like to acknowledge Osorio Hermanos & Cia for fabrication and maintenance of
383 the experimental HBOT chamber, also to Dr. Manuel Varas for providing the S6K1 antibody.

384

385 **References**

- 386 Barker, N. (2014). Adult intestinal stem cells: critical drivers of epithelial homeostasis and
387 regeneration. *Nature reviews Molecular cell biology*, 15(1), 19-33.
- 388 Basak, O., Beumer, J., Wiebrands, K., Seno, H., van Oudenaarden, A., & Clevers, H. (2017). Induced
389 quiescence of Lgr5+ stem cells in intestinal organoids enables differentiation of hormone-producing
390 enteroendocrine cells. *Cell stem cell*, 20(2), 177-190.
- 391 Benincasa, J. C., de Freitas Filho, L. H., Carneiro, G. D., Sielski, M. S., Giorgio, S., Werneck, C. C.,
392 & Vicente, C. P. (2019). Hyperbaric oxygen affects endothelial progenitor cells proliferation in vitro.
393 *Cell biology international*, 43(2), 136-146.
- 394 Benjamin, D., Colombi, M., Moroni, C., & Hall, M. N. (2011). Rapamycin passes the torch: a new
395 generation of mTOR inhibitors. *Nature reviews Drug discovery*, 10(11), 868.
- 396 Bennett, M. H., Trytko, B., & Jonker, B. (2012). Hyperbaric oxygen therapy for the adjunctive
397 treatment of traumatic brain injury. *Cochrane Database of Systematic Reviews*, (12).
- 398 Cappella, P., Gasparri, F., Pulici, M., & Moll, J. (2008). A novel method based on click chemistry,
399 which overcomes limitations of cell cycle analysis by classical determination of BrdU incorporation,
400 allowing multiplex antibody staining. *Cytometry Part A: the journal of the International Society for*
401 *Analytical Cytology*, 73(7), 626-636.
- 402 Clevers, H. (2013). The intestinal crypt, a prototype stem cell compartment. *Cell*, 154(2), 274-284.
- 403 Cox, L. S., & Mattison, J. A. (2009). Increasing longevity through caloric restriction or rapamycin
404 feeding in mammals: common mechanisms for common outcomes? *Aging Cell*, 8(5), 607-613.
- 405 Dai, D. F., Karunadharma, P. P., Chiao, Y. A., Basisty, N., Crispin, D., Hsieh, E. J., ... & Beyer, R.
406 P. (2014). Altered proteome turnover and remodeling by short-term caloric restriction or rapamycin
407 rejuvenate the aging heart. *Aging cell*, 13(3), 529-539.
- 408 Dave, K. R., Prado, R., Busto, R., Raval, A. P., Bradley, W. G., Torbati, D., & Perez-Pinzon, M. A.
409 (2003). Hyperbaric oxygen therapy protects against mitochondrial dysfunction and delays onset of
410 motor neuron disease in Wobbler mice. *Neuroscience*, 120(1), 113-120.
- 411 De Mey, J. R., & Freund, J. N. (2013). Understanding epithelial homeostasis in the intestine: an old
412 battlefield of ideas, recent breakthroughs and remaining controversies. *Tissue barriers*, 1(2), e24965.
- 413 Dejmek, J., Kohoutova, M., Kripnerova, M., Čedíková, M., Tůma, Z., Babuška, V., ... & Kuncova, J.
414 (2018). Repeated exposure to hyperbaric hyperoxia affects mitochondrial functions of the lung
415 fibroblasts. *Physiological Research*, 67.
- 416 Dhar, M., Nielsen, N., Beatty, K., Eaker, S., Adair, H., & Geiser, D. (2012). Equine peripheral blood-
417 derived mesenchymal stem cells: isolation, identification, trilineage differentiation and effect of
418 hyperbaric oxygen treatment. *Equine veterinary journal*, 44(5), 600-605.
- 419 Eskes, A. M., Ubbink, D. T., Lubbers, M. J., Lucas, C., & Vermeulen, H. (2011). Hyperbaric oxygen
420 therapy: solution for difficult to heal acute wounds? Systematic review. *World journal of surgery*,
421 35(3), 535-542.

422 Espey, M. G. (2013). Role of oxygen gradients in shaping redox relationships between the human
423 intestine and its microbiota. *Free Radical Biology and Medicine*, 55, 130-140.

424 Fingar, D. C., Richardson, C. J., Tee, A. R., Cheatham, L., Tsou, C., & Blenis, J. (2004). mTOR
425 controls cell cycle progression through its cell growth effectors S6K1 and 4E-BP1/eukaryotic
426 translation initiation factor 4E. *Molecular and cellular biology*, 24(1), 200-216.

427 Fingar, D. C., Salama, S., Tsou, C., Harlow, E. D., & Blenis, J. (2002). Mammalian cell size is
428 controlled by mTOR and its downstream targets S6K1 and 4EBP1/eIF4E. *Genes & development*,
429 16(12), 1472-1487.

430 Geng, C. K., Cao, H. H., Ying, X., & Yu, H. L. (2015). Effect of mesenchymal stem cells
431 transplantation combining with hyperbaric oxygen therapy on rehabilitation of rat spinal cord injury.
432 *Asian Pacific journal of tropical medicine*, 8(6), 468-473.

433 Hochmuth, C. E., Biteau, B., Bohmann, D., & Jasper, H. (2011). Redox regulation by Keap1 and Nrf2
434 controls intestinal stem cell proliferation in *Drosophila*. *Cell stem cell*, 8(2), 188-199.

435 Hu, J. K. H., Du, W., Shelton, S. J., Oldham, M. C., DiPersio, C. M., & Klein, O. D. (2017). An FAK-
436 YAP-mTOR signaling axis regulates stem cell-based tissue renewal in mice. *Cell stem cell*, 21(1),
437 91-106.

438 Igarashi, M., & Guarente, L. (2016). mTORC1 and SIRT1 cooperate to foster expansion of gut adult
439 stem cells during calorie restriction. *Cell*, 166(2), 436-450.

440 Ishihara, A. (2019). Mild hyperbaric oxygen: mechanisms and effects. *The Journal of Physiological
441 Sciences*, 69(4), 573-580.

442 Kalani, M., Jörneskog, G., Naderi, N., Lind, F., & Brismar, K. (2002). Hyperbaric oxygen (HBO)
443 therapy in treatment of diabetic foot ulcers: long-term follow-up. *Journal of Diabetes and its
444 Complications*, 16(2), 153-158.

445 Kranke, P., Bennett, M. H., Martyn-St James, M., Schnabel, A., Debus, S. E., & Weibel, S. (2015).
446 Hyperbaric oxygen therapy for chronic wounds. *Cochrane Database of Systematic Reviews*, (6).

447 Lane, J. D., Korolchuk, V. I., Murray, J. T., Rabanal-Ruiz, Y., & Otten, E. G. (2017). mTORC1 as
448 the main gateway to autophagy. *Essays in biochemistry*, 61(6), 565-584.

449 Lee, C. C., Chen, S. C., Tsai, S. C., Wang, B. W., Liu, Y. C., Lee, H. M., & Shyu, K. G. (2006).
450 Hyperbaric oxygen induces VEGF expression through ERK, JNK and c-Jun/AP-1 activation in
451 human umbilical vein endothelial cells. *Journal of biomedical science*, 13(1), 143-156.

452 Lehner, B., Sandner, B., Marschallinger, J., Lehner, C., Furtner, T., Couillard-Despres, S., ... &
453 Aigner, L. (2011). The dark side of BrdU in neural stem cell biology: detrimental effects on cell cycle,
454 differentiation and survival. *Cell and tissue research*, 345(3), 313.

455 Matchett, G. A., Martin, R. D., & Zhang, J. H. (2009). Hyperbaric oxygen therapy and cerebral
456 ischemia: neuroprotective mechanisms. *Neurological Research*, 31(2), 114-121.

457 Muñoz, J., Stange, D. E., Schepers, A. G., Van De Wetering, M., Koo, B. K., Itzkovitz, S., ... &
458 Myant, K. (2012). The Lgr5 intestinal stem cell signature: robust expression of proposed quiescent
459 '+ 4' cell markers. *The EMBO journal*, 31(14), 3079-3091.

460 Murakami, M., Ichisaka, T., Maeda, M., Oshiro, N., Hara, K., Edenhofer, F., ... & Yamanaka, S.
461 (2004). mTOR is essential for growth and proliferation in early mouse embryos and embryonic stem
462 cells. *Molecular and cellular biology*, 24(15), 6710-6718.

463 Newton, P. T., Li, L., Zhou, B., Schweingruber, C., Hovorakova, M., Xie, M., ... & Suter, S. (2019).
464 A radical switch in clonality reveals a stem cell niche in the epiphyseal growth plate. *Nature*,
465 567(7747), 234-238.

466 Peña-Villalobos, I., Casanova-Maldonado, I., Lois, P., Prieto, C., Pizarro, C., Lattus, J., ... & Palma,
467 V. (2018). Hyperbaric oxygen increases stem cell proliferation, angiogenesis and wound-healing
468 ability of WJ-MSCs in diabetic mice. *Frontiers in physiology*, 9, 995.

469 Peña-Villalobos, I., Casanova-Maldonado, I., Lois, P., Sabat, P., & Palma, V. (2019). Adaptive
470 physiological and morphological adjustments mediated by intestinal stem cells in response to food
471 availability in mice. *Frontiers in physiology*, 9, 1821.

472 Ren, J., Tang, C. Z., Li, X. D., Niu, Z. B., Zhang, B. Y., Zhang, T., ... & Wang, F. C. (2018).
473 Identification of G2/M phase transition by sequential nuclear and cytoplasmic changes and molecular
474 markers in mice intestinal epithelial cells. *Cell Cycle*, 17(6), 780-791.

475 Sampson, L. L., Davis, A. K., Grogg, M. W., & Zheng, Y. (2015). mTOR disruption causes intestinal
476 epithelial cell defects and intestinal atrophy postinjury in mice. *The FASEB Journal*, 30(3), 1263-
477 1275.

478 Saxton, R. A., & Sabatini, D. M. (2017). mTOR signaling in growth, metabolism, and disease. *Cell*,
479 168(6), 960-976.

480 Schieke, S. M., Phillips, D., McCoy, J. P., Aponte, A. M., Shen, R. F., Balaban, R. S., & Finkel, T.
481 (2006). The mammalian target of rapamycin (mTOR) pathway regulates mitochondrial oxygen
482 consumption and oxidative capacity. *Journal of Biological Chemistry*, 281(37), 27643-27652.

483 Shyh-Chang, N., & Ng, H. H. (2017). The metabolic programming of stem cells. *Genes &
484 development*, 31(4), 336-346.

485 Snippert, H. J., Van Der Flier, L. G., Sato, T., Van Es, J. H., Van Den Born, M., Kroon-Veenboer,
486 C., ... & Clevers, H. (2010). Intestinal crypt homeostasis results from neutral competition between
487 symmetrically dividing Lgr5 stem cells. *Cell*, 143(1), 134-144.

488 Sunkari, V. G., Lind, F., Botusan, I. R., Kashif, A., Liu, Z. J., Ylä-Herttuala, S., ... & Catrina, S. B.
489 (2015). Hyperbaric oxygen therapy activates hypoxia-inducible factor 1 (HIF-1), which contributes
490 to improved wound healing in diabetic mice. *Wound Repair and Regeneration*, 23(1), 98-103.

491 Thom, S. R., Bhopale, V. M., Velazquez, O. C., Goldstein, L. J., Thom, L. H., & Buerk, D. G. (2006).
492 Stem cell mobilization by hyperbaric oxygen. *American Journal of Physiology-Heart and Circulatory
493 Physiology*.

494 Totafurno, J. O. H. N., Bjerknes, M., & Cheng, H. A. Z. E. L. (1987). The crypt cycle. Crypt and
495 villus production in the adult intestinal epithelium. *Biophysical journal*, 52(2), 279-294.

496 Tothova, Z., Kollipara, R., Huntly, B. J., Lee, B. H., Castrillon, D. H., Cullen, D. E., ... & Armstrong,
497 S. A. (2007). FoxOs are critical mediators of hematopoietic stem cell resistance to physiologic
498 oxidative stress. *Cell*, 128(2), 325-339.

499 Wang, T., Tsui, B., Kreisberg, J. F., Robertson, N. A., Gross, A. M., Yu, M. K., ... & Ideker, T.
500 (2017). Epigenetic aging signatures in mice livers are slowed by dwarfism, calorie restriction and
501 rapamycin treatment. *Genome biology*, 18(1), 57.

502 Wang, X. L., Yang, Y. J., Xie, M., Yu, X. H., Liu, C. T., & Wang, X. (2007). Proliferation of neural
503 stem cells correlates with Wnt-3 protein in hypoxic-ischemic neonate rats after hyperbaric oxygen
504 therapy. *Neuroreport*, 18(16), 1753-1756.

505 Wei, P., Dove, K. K., Bensard, C., Schell, J. C., & Rutter, J. (2018). The force is strong with this one:
506 metabolism (over) powers stem cell fate. *Trends in cell biology*, 28(7), 551-559.

507 Wei, Y., Yu, L., Bowen, J., Gorovsky, M. A., & Allis, C. D. (1999). Phosphorylation of histone H3
508 is required for proper chromosome condensation and segregation. *Cell*, 97(1), 99-109.

509 Yilmaz, Ö. H., Katajisto, P., Lamming, D. W., Gültekin, Y., Bauer-Rowe, K. E., Sengupta, S., ... &
510 Nielsen, G. P. (2012). mTORC1 in the Paneth cell niche couples intestinal stem-cell function to
511 calorie intake. *Nature*, 486(7404), 490.

512 Zhang, T., Yang, Q. W., Wang, S. N., Wang, J. Z., Wang, Q., Wang, Y., & Luo, Y. J. (2010).
513 Hyperbaric oxygen therapy improves neurogenesis and brain blood supply in piriform cortex in rats
514 with vascular dementia. *Brain injury*, 24(11), 1350-1357.

515 Zhang, X. Y., Yang, Y. J., Xu, P. R., Zheng, X. R., Wang, Q. H., Chen, C. F., & Yao, Y. (2011). The
516 role of β -catenin signaling pathway on proliferation of rats neural stem cells after hyperbaric oxygen
517 therapy in vitro. *Cellular and molecular neurobiology*, 31(1), 101-109.

518

519

520

521

522

523

524

525

526

527

528

529

530

531

532

533 **Declarations**

534

535 Consent for publication: Not applicable

536 Availability of data and material: All data is available as figures or supplementary information

537 Funding: Work was supported by FONDEF grant D09E1047 (VP), FONDECYT Postdoctoral

538 3180108 (IPV) and FONDECYT grant 1110237 and 1140697 (VP).

539 Author contributions

540 **Conceptualization:** ICM, VP & IPV

541 **Investigation:** ICM, IPV & PL

542 **Formal Analysis:** ICM & IPV

543 **Writing-Original Draft:** ICM; IPV & DA

544 **Writing-Review & Editing:** VP & PL

545 **Supervision:** VP

546 Declaration of interests: The authors declare no competing financial interests.

547 Ethical standards: All procedures performed to elaborate this manuscript comply with the Chilean

548 legislation and were approved by Institutional and Bioethical Use Committees (University of Chile).

Figures

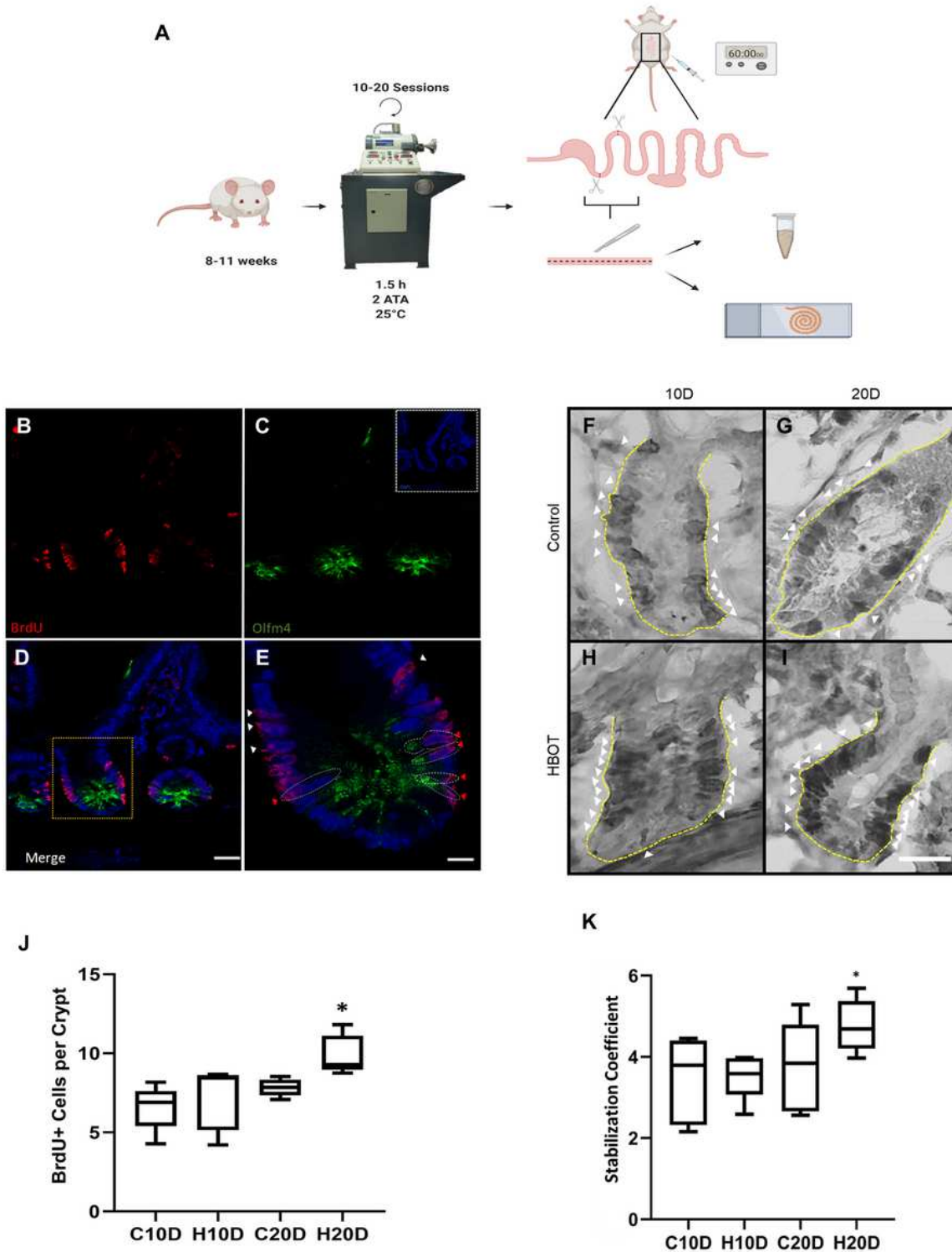


Figure 1

HBOT increases ISC proliferation in a synchronous fashion. A) Schematic workflow of HBOT treatment and experimental procedures on small intestine samples. B-E) Representative immunofluorescence images of ISC proliferation in intestinal crypts. B) Proliferative cells were detected by BrdU labeling (Red).

C) ISCs labeled as Olfm4+ cells, a cytoplasmatic marker (Green). Inset shows DAPI nuclear staining (Blue). D) Merged image. Yellow box indicates crypt with proliferating ISCs among other cell populations. Bar= 15 gm. E) Zoom of yellow box from image D. Red arrowheads indicate proliferating ISCs while white arrowheads indicate other proliferating cells within the intestinal crypt. Bar= 30 gm. F-G) Representative immunohistochemistry images of intestinal crypts with proliferating BrdU+ cells; experimental groups as indicated. Nuclei labeled by hematoxylin counterstaining. Bar= 20 gm. Yellow dotted lines outline the crypts while white arrowheads show BrdU+ cells. 1) Quantification of BrdU+ cells per crypt for each treatment. Asterisk indicate statistical significance. Permutation test. pc 0.05. n=5. K) Stabilization coefficient indicating the level of variation inside each group. Asterisk indicates statistical significance. Only H2OD shows significant differences, indicating synchronicity. Permutation test. p<0.05. n= 4.

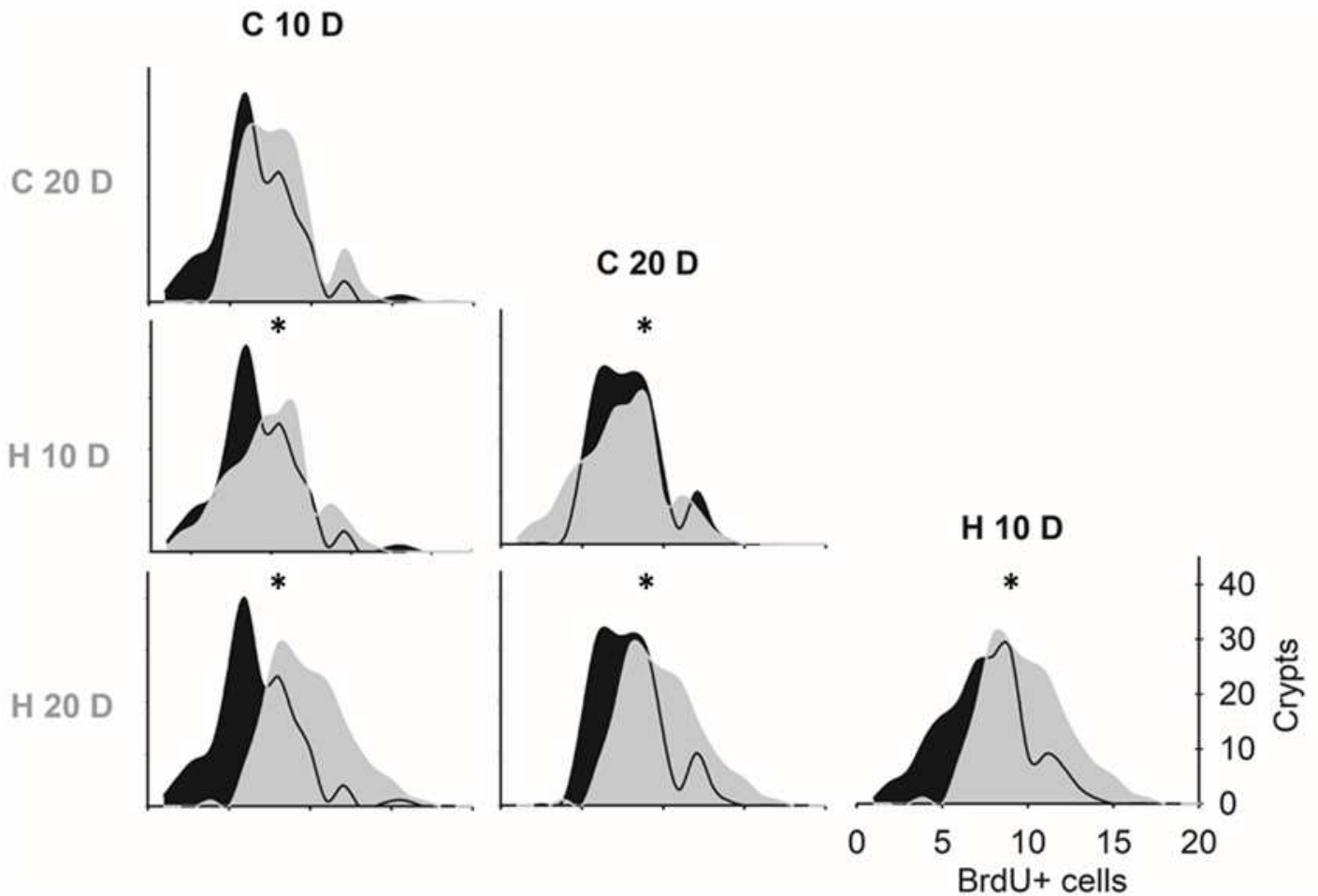


Figure 2

HBOT has an accumulative effect on time. Comparison of frequency distribution of BrdU+ cells per crypt between groups as indicated. Asterisk indicates differences ($p < 0,05$). Kohnogorov-Smimov test. Only the comparison between control groups shows no differences. n=4.

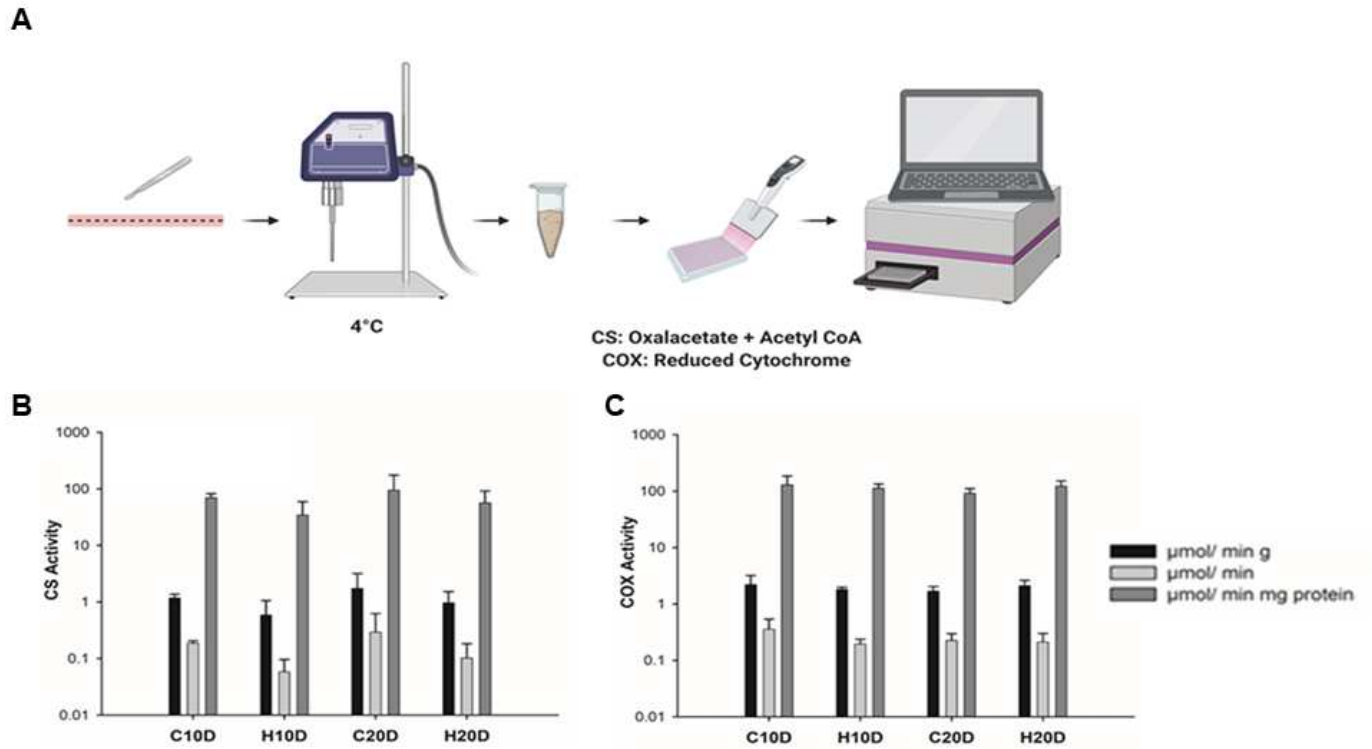


Figure 3

Aga. SNOT does not affect enzyme activity in the small intestine. A) Workflow of enzymatic assay for CS and COX activity in small intestine tissue. B) Bar graph of CS activity (µmol/min) under each treatment. No significant differences were found ($p > 0.05$). $n = 3$. C) COX activity (µmol/min) under each treatment. No significant differences were found. Black bars indicate activity per gram of tissue, dark grey bars indicate activity per total proteins in the sample and light grey bars indicate total activity. ($p = 0.135$). $n = 3$.

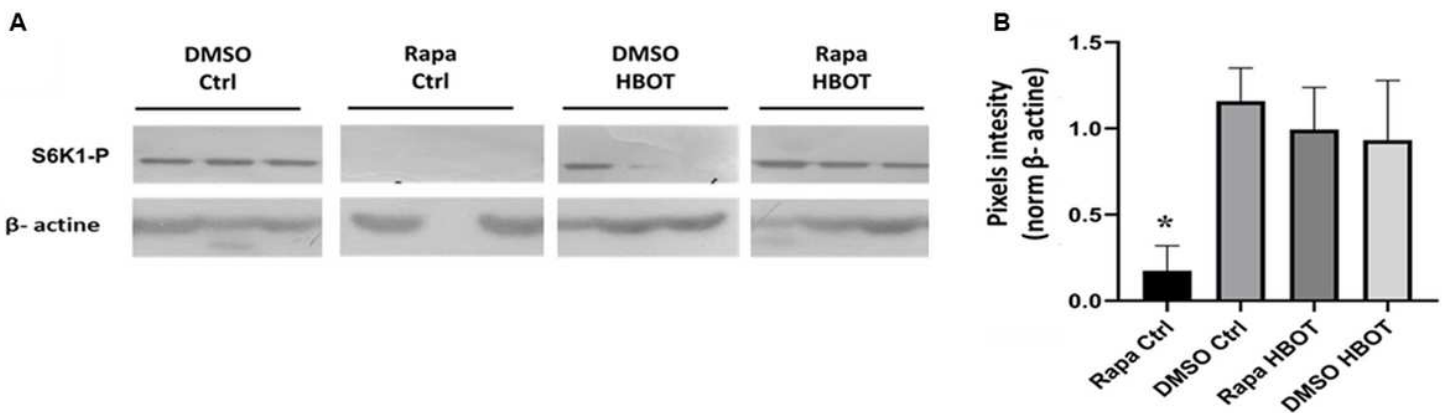


Figure 4

HBOT restores rapamycin-induced mTOR pathway inhibition. A) Western blot for phosphorylated S6101 (S6K1.14) and β-actin in each experimental group (triplicate). First row shows DMSO control group. Second row shows rapamycin control group. Third row shows rapamycin and HBOT group. Last row

shows DMSO and MOT group. SPOT sessions for 20 days. B) Quantification of pixel Wensity for SCr141-P presence in each group normalized with internal control p.n.s. Asterisks indicates statistical significance. Permutation hst.p<0.05, r, 2 per grow.

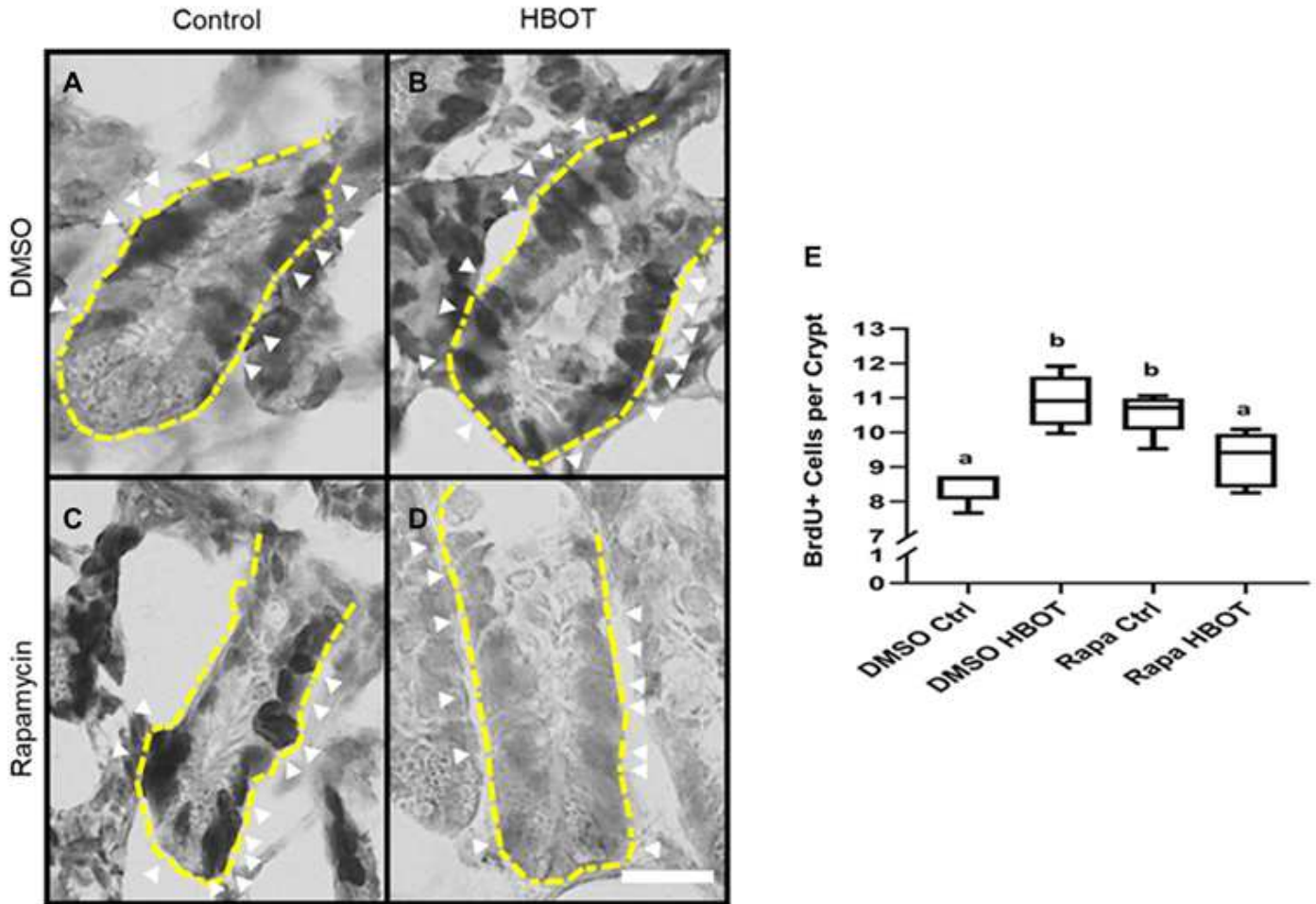


Figure 5

HBOT and rapamycin increase ISC proliferation independently. A-D) Representative immunohistochemistry images for proliferating cells, labeled by BrdU incorporation, in intestinal crypts for each experimental group. 20 days of treatment in each group. Nuclei labeled by hematoxylin counterstaining. Bar— 20 μ m. Yellow dotted lines outline the crypt periphery. White arrowheads show BrdU+ cells. E) Quantification of BrdU+ cells for each treatment. Same letters indicate no statistical significance while different letters indicate statistical significance. Permutation test. p<0.05. 11-5 per group.

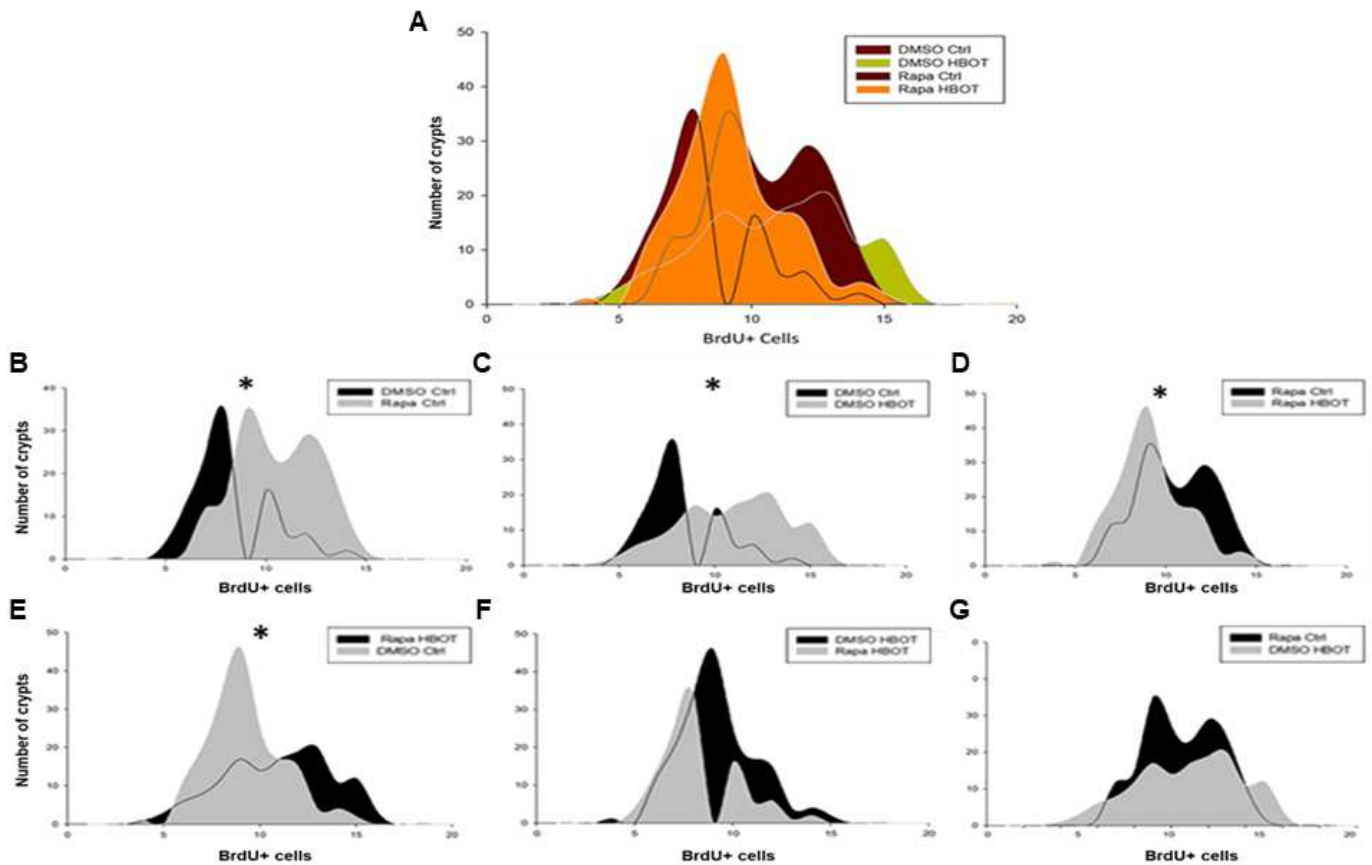


Figure 6

HBDE can simulate a caloric restriction. A) Superposition of frequency distribution for each Reap. All comparison was made by a KolmogorovsSmirnov test. B) Comparison between DMSO CPI and Rape Cid. pm 0.004 C) Comparison between DMSO CU) and DMSO 1180T. m 0.003 D) Comparison between Rape CPI and Raper BOOT. m 0.013 E) Comparison between DMSO Cirl and Rape BOOT. 0.009 r) Comparison between Rape 11BOT and DMSO Ctd. $p > 0.05$ G) Comparison between Raper Crd end DMSO 11BOT. $p > 0.05$. n= 5.

Supplementary Files

This is a list of supplementary files associated with this preprint. Click to download.

- [SF1.tif](#)